Topological estimation of percolation thresholds

Richard A. Neher[1]‡**, Klaus Mecke**[2] **and Herbert Wagner**[1]

[1] Arnold-Sommerfeld-Center for Theoretical Physics, LMU München, Theresienstrasse 37, 80333 München, Germany.
[2] Institut für Theoretische Physik, Universität Erlangen-Nürnberg, Staudtstraße 7, 91058 Erlangen, Germany.

E-mail: neher@kitp.ucsb.edu

Abstract. Global physical properties of random media change qualitatively at a percolation threshold, where isolated clusters merge to form one infinite connected component. The precise knowledge of percolation thresholds is thus of paramount importance. For two dimensional lattice graphs, we use the universal scaling form of the cluster size distributions to derive a relation between the mean Euler characteristic of the critical percolation patterns and the threshold density p_c. From this relation, we deduce a simple rule to estimate p_c, which is remarkably accurate. We present some evidence that similar relations might hold for continuum percolation and percolation in higher dimensions.

‡ Present address: KITP, University of California, Santa Barbara.

Consider a regular d-dimensional lattice where a fraction of sites is selected independently with probability p and deemed 'black', with the complementary vertices said to be white. The aggregate of these spatial lattice elements forms a random pattern, which we may partition into clusters after specifying a neighborhood. This simple set-up constitutes the standard model of Bernoullian percolation theory, and is applied to problems as diverse as transport in disordered media, epidemics, and the quark confinement transition in the early universe [1, 2, 3]. The central result of this theory is the existence of a sharp threshold value $0 < p_c < 1$ in an infinite lattice of dimension $d > 1$: When p increases across p_c, a single infinite cluster appears almost surely and grows in mass with increasing p beyond p_c [4, 5, 6].

Research in percolation theory focussed predominantly on the *universal* critical phenomena showing up in the vicinity of the threshold. On the other hand, for practical application of percolation concepts, it is the specific and *non-universal* value of p_c which is of primary importance. Exact values of p_c are known only for special classes of 2-d lattices [7, 8, 9, 10, 11, 12]. In all other cases, values of p_c are estimated numerically with computer simulations, which often are time consuming, in particular in three or higher dimensional lattices.

Here, we investigate the signature of the percolation transition in the *Euler Characteristic* of the spatial pattern formed by the percolating clusters. Its mean value per site, $\chi(p)$, provides a topological descriptor, which for a lattice Λ turns out to be an exactly calculable finite polynomial in p. For 2d-lattices the polynomials $\chi(p)$ have one non-trivial zero $0 < p_0(\Lambda) < 1$. From the comparison with known threshold values, we observe that $p_0(\Lambda)$ gives a tight upper bound for $p_c(\Lambda)$ for many lattices, but we also find exceptions to this rule-of-thumb. In the case of 3d-lattices, each $\chi(p)$-polynomial has two distinct nontrivial zeros which are again slightly larger than the thresholds values of the two distinct percolation transitions of black and white clusters.

For 2d-lattices, we explain this peculiar ordering of p_0 and p_c using the known scaling expression for the critical percolation clusters at p_c. Moreover, this approach leads to a surprisingly simple relation which combines via $\chi(p)$ the specific lattice geometry with universal critical percolation features into an accurate *parameter-free* estimate of percolation thresholds of all 2d-lattices considered in this note. Our work also applies to bond percolation problems when they are reformulated as the equivalent site percolation problem on the covering lattice.

1. The Euler characteristic in percolation theory

The percolation transition is a paradigm of a non-thermal phase transition, where the local merging of black clusters causes an abrupt change in the large scale-connectivity of black vertices. Since the Euler Characteristic (EC) is a prominent descriptor of global aspects of spatial patterns, we may expect it to be also a valuable tool in the study of the percolation transition. In this section, we introduce the EC descriptively and discuss its salient features; a more technical but elementary outline can be found in the supplementary notes.

For the time being we consider planar lattices with cyclic boundary conditions. The basic object in site percolation are clusters of vertices, naturally defined by the connectivity of the host lattice: Two black vertices belong to the same cluster if they are joined by a path of black nearest-neighbors on the lattice. Moreover, each configuration of black clusters specifies in a natural way an aggregate of white clusters

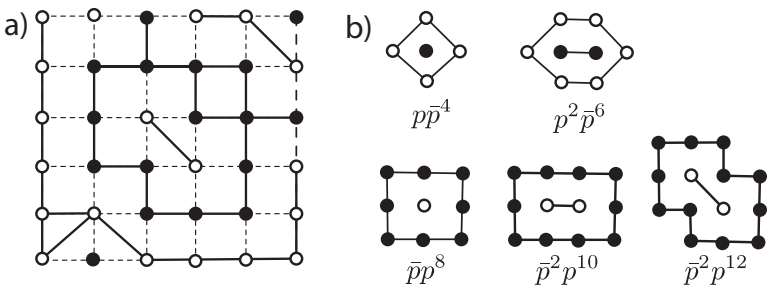

Figure 1. a) Black clusters partition the white vertices into an aggregate of complementary clusters. For the square lattice, white vertices are connected by lattice bonds *and* by diagonal bonds across the faces of the lattice. b) The black and white clusters of size 1 and 2 on the square lattice. The white perimeter sites of a black cluster are connected (and vice versa).

with a complementary neighborhood, which is in general distinct from the black one; it may be visualized by drawing "matching" bonds diagonally across polygonal faces of the host lattice, as illustrated in Figure 1a for the square lattice. The lattice comprising the vertices of the original lattice and all bonds between neighboring white vertices is called the *matching lattice*. The complementary connectivities of black and white clusters imply, that the white perimeter vertices of black clusters form closed boundaries of holes in white clusters and vice versa, as illustrated for black and white clusters of size one and two in Figure 1b. The percolation thresholds of a lattice Λ and its matching lattice $\bar{\Lambda}$ add up to one [13]

$$p_c(\Lambda) + p_c(\bar{\Lambda}) = 1, \tag{1}$$

implying that the black and white clusters are simultaneously critical at $p = p_c$.

Let g_{st} denote the number of black clusters per lattice site with a fixed size s and a fixed number t of perimeter vertices. The mean density of finite black clusters is then given by $n(p) = \sum_s n_s(p) = \sum_{st} p^s g_{st} \bar{p}^t$, where $\bar{p} = 1 - p$ is the density of white vertices, comp. Figure 1b. Correspondingly, the mean density of the complementary finite white clusters reads $\bar{n}(\bar{p}) = \sum_s \bar{n}_s(\bar{p}) = \sum_{st} \bar{p}^s \bar{g}_{st} p^t$. In their pioneering paper [13] on exact percolation thresholds in two dimensions, Sykes and Essam considered the difference

$$\chi(p) := n(p) - \bar{n}(\bar{p}) = -\bar{\chi}(\bar{p}) \tag{2}$$

and found that $\chi(p)$ is a finite polynomial, which they called *matching polynomial*. This observation enabled them to obtain, for instance, the exact critical probability of site percolation on the "self-matching" triangular lattice from $\chi_{tri}(p_c) = 0$ at $p_c = \frac{1}{2}$.

When specialized to spatial patterns P_N on a planar lattice with N sites, the definition of the Euler characteristic, $\mathcal{X}$, reads

$$\mathcal{X}(P_N) = \#\text{ clusters of } P_N - \#\text{ holes in } P_N. \tag{3}$$

From comparison of this definition with Equation 2, and the observation that complementary (finite) white clusters constitute the holes in black clusters (see above), we see that the matching polynomial $\chi(p)$ may be identified with the mean Euler characteristic per site (MEC) of the black clusters, $\chi(p) = \lim_{N\to\infty} \langle \frac{1}{N} \mathcal{X}(P_N) \rangle_p$. Equation 2 expresses the fundamental topological invariance of the EC, but the representation as the difference of two infinite series is not convenient for practical

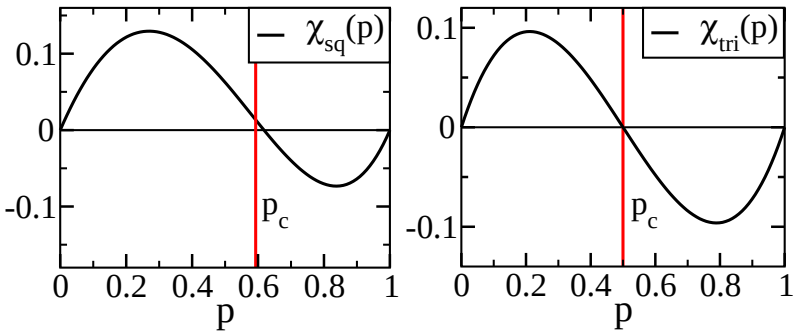

Figure 2. The MEC of the square lattice (left) and of the triangular lattice (right). Note, that p_0 is slightly above p_c for the square lattice. The triangular lattice is self-matching and $p_c = p_0 = 1/2$.

computation. For that purpose we employ Euler's polyhedral formula, which expresses the EC

$$\mathcal{X} = \#v - \#e + \#f \tag{4}$$

in terms of the number of black vertices $\#v$, edges joining black vertices $\#e$ and polygonal faces with black boundary $\#f$, respectively. The mean value $\chi(p)$ is now obtained by a simple local calculation. As an example, consider the square lattice: (i) A vertex is black with probability p. (ii) The two vertices bounding an edge are black with probability p^2, and there are two edges per vertex. (ii) The four vertices surrounding a face are black with probability p^4. Hence, we find for the square lattice

$$\chi_{sq}(p) = p - 2p^2 + p^4. \tag{5}$$

The graph of $\chi_{sq}(p)$ is shown in Figure 2a. Analogously, one finds for the triangular lattice $\chi_{tri}(p) = p - 3p^2 + 2p^3$, which has the above mentioned self-matching property $\chi(p) = -\bar{\chi}(1-p)$ (see Figure 2b). Whenever the lattices cells have finite number of boundary vertices, $\chi(p)$ is a finite polynomial.

The graph of $\chi_{sq}(p)$ in Figure 2 is typical for the MEC of 2d-lattices. At small values of p, black clusters are *finite* holes in a *single infinite white* cluster. As long as p is well below p_c, the density of holes within the small-sized black clusters is negligible, hence $\chi(p)$ is positive and increases with increasing p. On the other hand, for $p > p_c$, and $1 - p \ll 1$, there is a *single infinite black* cluster with *finite* (white) holes and thus $\chi(p) < 0$, in accordance with Equation 3. In the intermediate range of p, which includes p_c, the MEC decreases as the black clusters grow in size and merge to generate a single infinite component as p passes the percolation threshold at p_c. We see that the typical features of the MEC are governed by the interplay of the complementary finite black and white clusters. The percolation transition with the singular emergence of an infinite cluster leaves its signature only in the zero crossing of $\chi(p)$ at $0 < p_0 < 1$ with a value of p_0 expected to be comparable with p_c.

2. Percolation thresholds and the zero crossing of the MEC

The idea that the zero crossing of the MEC should occur near the critical probability p_c is plausible and is supported, for instance, by the fact that $p_0 = p_c = 1/2$ for site percolation on the self-matching triangular lattice, but it calls for a more precise and

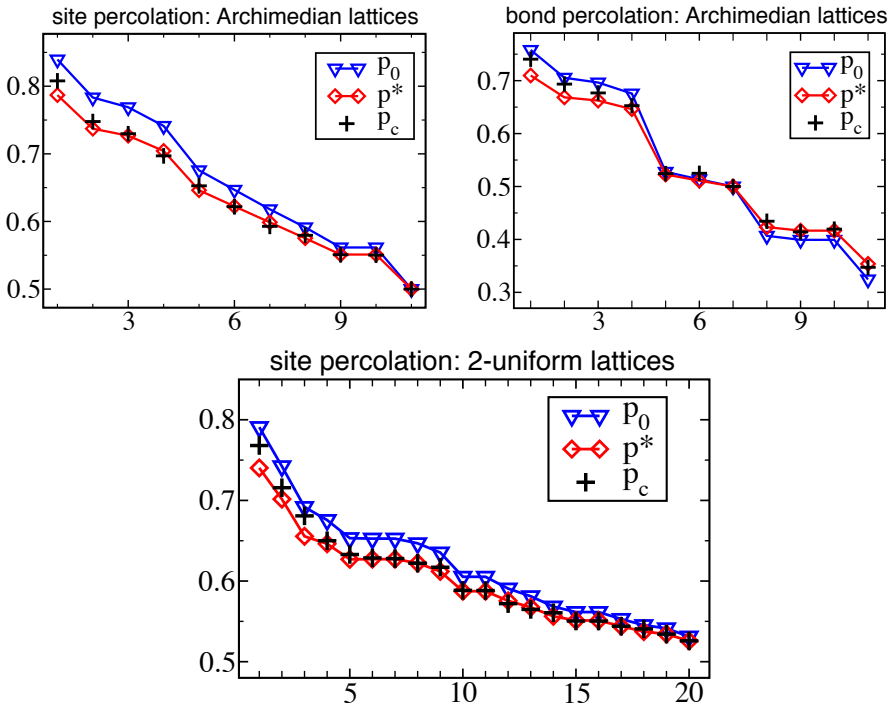

Figure 3. The percolation threshold p_c is slightly below the zero crossing p_0 of the MEC whenever $p_c > \frac{1}{2}$. This order is reversed, if $p_c < \frac{1}{2}$, as apparent in the panel on bond percolation. The solution p^* of Equation 18 provides a very accurate estimate of p_c. The deviation $|p_c - p^*|$ exceeds 0.01 only for very open lattices with high percolation thresholds. Lattices are in the order of decreasing percolation threshold. For vertex configurations, numerical values of p_c and p^* for the 2-uniform lattices, see Tab. 1 in the supplementary material. Numerical estimates of p_c^{site} for the Archimedean lattices are taken from [14], values for p_c^{bond} are from [15, 16].

quantitative argument. Here we will first compare p_0 with p_c and we shall find that p_0 provides generally a tight upper bound to p_c whenever $p_c > 1/2$.

2.1. Archimedean lattices

To begin with, we consider the eleven Archimedean lattices, where all vertices are equivalent up to a symmetry operation and all faces are regular polygons. The most prominent members of this class are the triagonal, the square, the honeycomb and the kagomé lattice. Each lattice is uniquely characterized by the number of edges n_i of the polygons surrounding a vertex [17]. A lattice of coordination number z is therefore conveniently denoted by the symbols $(n_1, \ldots, n_z)$, where a_i identical consecutive polygons are often abbreviated as $n_i^{a_i}$. For example, a vertex of the square lattice is surrounded by four squares. The vertex type of the square lattice is therefore $(4, 4, 4, 4)$ or (4^4) in the abbreviated notation. Similarly, the a vertex of the kagomé lattice is surrounded by alternating triangles and hexagons and has vertex type $(3, 6, 3, 6)$. With this notation, the MECs of the Archimedean lattices are given

by

$$\chi(p) = p(1-p)\left(1 - p\sum_{i=1}^{z}\frac{1}{n_i}\sum_{\mu=0}^{n_i-3}p^{\mu}\right). \tag{6}$$

The percolation thresholds of Archimedean lattices are known to very high precision [14]. In Figure 3, we compare p_c to the zero crossing p_0 of $\chi(p)$. For the self-matching triangular lattice $p_0 = p_c = \frac{1}{2}$. Furthermore, a close relation appears to exist between p_c and p_0 even for lattices with $p_c > \frac{1}{2}$: p_c is bounded from above by p_0, with $p_0 - p_c$ increasing steadily with $p_c - \frac{1}{2}$. Similar observations can be made for the duals of the Archimedean lattices, see Fig. 2 of the supplementary material.

2.2. 2-uniform lattices

Next, we study the larger class of 2-uniform lattices, which again consist of regular polygons but have two distinct vertex types [17]. The two vertex types can occur with different abundances, and a 2-uniform lattice is commonly denoted by $s_1(n_1^1, \ldots, n_{z_1}^1) + s_2(n_1^2, \ldots, n_{z_2}^2)$, where s_i is the fraction of vertices that are of type i. The MECs are given by the straightforward generalization of Equation 6

$$\chi(p) = p(1-p)\left(1 - p\sum_{\nu=1,2}\sum_{i=1}^{z_\nu}\frac{s_\nu}{n_i^\nu}\sum_{\mu=0}^{n_i^\nu-3}p^{\mu}\right), \tag{7}$$

which can obviously be generalized to any finite number of vertex types. We are not aware that the percolation thresholds of 2-uniform lattices have been previously determined, and we therefore estimated them using an algorithm adopted from [18]. Again, p_0 provides a tight upper bound to p_c as shown in Figure 3. The vertex configurations, as well as p_0 and the estimate of p_c for the 2-uniform lattices are given in Table 4 of the supplementary material.

2.3. Bond percolation in two dimensions

Every bond percolation problem is equivalent to site percolation on the covering lattice. The covering lattices, however, are not necessarily planar but decorated mosaics. A decorated mosaic is constructed from a planar lattice, where in a subset of the faces all diagonal connection have been added (the face is decorated). A pair of lattices where complementary sets of faces are decorated constitute a pair of matching lattices in the sense of Equation 1 [13]. Calculating the MEC of decorated mosaics is slightly more laborious, but a general framework for the calculation has been presented in ref. [19]. Using this framework, we calculated the MEC of the covering lattices of all Archimedean lattices with vertex $(n_1, \ldots, n_z)$

$$\chi(p) = -p + \frac{2}{z}\left(1 - (1-p)^z\right) + \sum_i \frac{2}{zn_i}p^{n_i}. \tag{8}$$

Comparing numerical estimates of p_c [15, 16] to p_0 confirms $p_0 > p_c$ if $p_c > \frac{1}{2}$ (Figure 3), albeit with one notable exception for the lattice 6 with vertex configuration $(3, 4, 6, 4)$. For lattices with $p_c < \frac{1}{2}$ the order of p_c and p_0 is reversed, as expected from the matching properties of p_c and $\chi(p)$.

The relation between p_c and p_0 is not restricted to regular lattices but also holds for the quasi-periodic Penrose tiling and random tessellations of the plane such as Voronoi and Delauny tessellations, see supplementary material for values of p_c and p_0 and the polynomials of the MECs.

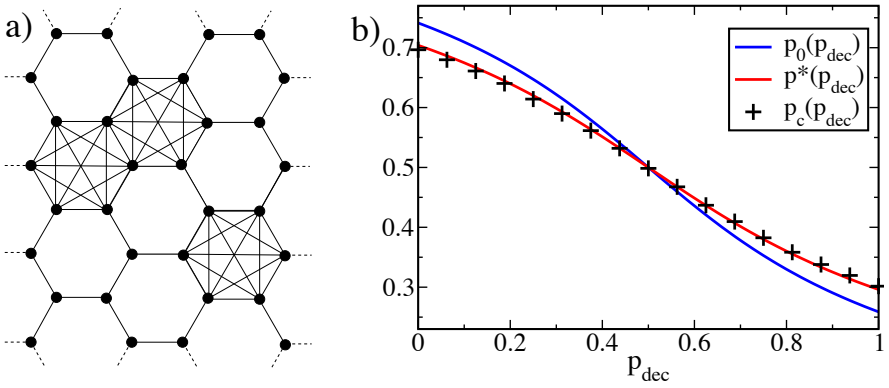

Figure 4. a) A lattice face is decorated, when all diagonal connections across the faces have been added to the lattice graph, as illustrated here for three faces of the hexagonal lattice. We consider randomly decorated lattices where each face is decorated with probability p_{dec}. b) The site percolation threshold $p_c(p_{dec})$ decreases smoothly as the degree of decoration is varied from $p_{dec} = 0$ to $p_{dec} = 1$. The zero crossing $p_0(p_{dec})$ of $\chi(p, p_{dec})$ provides a tight upper to $p_c(p_{dec})$ if $p_c(p_{dec}) > \frac{1}{2}$ and vice versa. The solution of Equation 18, $p^*(p_{dec})$, lies within 0.005 of $p_c(p_{dec})$ with the largest deviations at full or no decoration.

2.4. Randomly decorated mosaics

Instead of regular decorated mosaics, we now consider lattices where each face is decorated with probability p_{dec}, as illustrated in Figure 4a. We are not aware that this type of percolation process, which bears some similarity to a bond-site percolation processes, has been studied before. Our numerical estimates of percolation thresholds of a randomly decorated mosaic decreases smoothly from $p_c(p_{dec} = 0)$ to $p_c(p_{dec} = 1)$, in accord with the containment property [20]. Randomly decorated lattices fulfill the statistical matching property $p_c(p_{dec}) + p_c(1 - p_{dec}) = 1$, from which $p_c(0.5) = 0.5$ follows. The averaging over the different decoration states of the lattice is straightforward and the MEC of randomly decorated mosaics can be calculated in the same way as that of regular decorated mosaics. For the hexagonal lattice one finds

$$\chi(p, p_{dec}) = (1 - p_{dec})\chi_{hex}(p) + p_{dec}\bar{\chi}_{hex}(p). \tag{9}$$

From Equation 2 follows the symmetry relation $\chi(p, p_{dec}) = -\chi(1-p, 1-p_{dec})$. Hence, we have $p_0(p_{dec}) + p_0(1-p_{dec}) = 1$ in analogy to $p_c(p_{dec}) + p_c(1-p_{dec}) = 1$. Our results for the randomly decorated hexagonal lattice are shown in Figure 4b. The zero crossing $p_0(p_{dec})$ follows $p_c(p_{dec})$ very closely, being a tight upper bound for $p_{dec} > \frac{1}{2}$ and a lower bound otherwise. Similar results can be obtained for other Archimedean lattices (data not shown).

3. The EC of critical percolation and estimation of $p_c(\Lambda)$

In the previous sections, we saw that $p_c(\Lambda)$ – a global property of the lattice – is followed rather closely by $p_0(\Lambda)$, a locally computable quantity. Here, we are going to explore the relation of $p_c(\Lambda)$ with $p_0(\Lambda)$ in more detail by evoking a generally accepted scaling form for the densities $n_s(p)$ of large clusters at p_c [21]. These densities

determine $\chi(p)$ according to Equation 2. Moreover, they also enter in the sum rules [4]

$$p = \sum_s s n_s(p) + P_\infty(p), \quad \bar{p} = \sum_s s \bar{n}_s(\bar{p}) + \bar{P}_\infty(\bar{p}), \tag{10}$$

which express the probability for a particular vertex to be black (p) or white ($\bar{p}$).

In 2d-lattice graphs only a single critical point exists, so that $P_\infty(p_c) = 0 = \bar{P}_\infty(\bar{p}_c)$. At the threshold the scaling ansatz reads

$$n_s(p_c) \simeq a(\Lambda) s^{-\tau} \quad \text{and} \quad \bar{n}_s(\bar{p}_c) \simeq \bar{a}(\bar{\Lambda}) s^{-\tau}. \tag{11}$$

The non-universal amplitudes $a(\Lambda)$ and $\bar{a}(\bar{\Lambda})$ account for the particular structure of the underlying lattice and its matching partner, whereas the value of the universal exponent $\tau = 187/91$ is known exactly in two dimensions [4, 22, 23].

In order to exploit the scaling hypothesis, we define

$$\chi_{s_0}(p) := \chi(p) - \sum_{s=1}^{s_0} \left[n_s(p) - \bar{n}_s(\bar{p}) \right], \tag{12}$$

and set

$$\chi_{s_0}(p_c) \simeq (a - \bar{a}) \sum_{s > s_0} s^{-\tau}. \tag{13}$$

Likewise,

$$\Delta_{s_0}(p) \ := (p - \bar{p}) - \sum_{s=1}^{s_0} s \left[n_s(p) - \bar{n}_s(\bar{p}) \right]; \tag{14}$$

$$\Delta_{s_0}(p_c) \simeq \ (a - \bar{a}) \sum_{s > s_0} s^{1-\tau}. \tag{15}$$

After elimination of the non-universal scaling amplitudes, we arrive at

$$\chi_{s_0}(p_c) \simeq \frac{\zeta(\tau, s_0)}{\zeta(\tau - 1, s_0)} \Delta_{s_0}(p_c), \tag{16}$$

where $\zeta(\tau, s_0) = \sum_{s=1}^{\infty} (s + s_0)^{-\tau}$ is the Riemann Zeta-function with offset s_0.

The relation (16) may be applied as an equality, for instance, (i) to determine a value of s_0 from the requirement that the left- and right-hand sides equalize within a prescribed accuracy, or (ii) to estimate $p_c(\Lambda)$. For the latter purpose, we rewrite Equation 16 by substituting the defining expressions (13, 15) for $\chi_{s_0}(p)$ and $\Delta_{s_0}(p)$. The result is

$$\begin{aligned} \chi(p) = \frac{\zeta(\tau, s_0)}{\zeta(\tau - 1, s_0)} \left[(2p - 1) - \sum_{s=1}^{s_0} s \left[n_s(p) - \bar{n}_s(\bar{p}) \right] \right] \\ + \sum_{s=1}^{s_0} \left[n_s(p) - \bar{n}_s(\bar{p}) \right]. \end{aligned} \tag{17}$$

The real root, $\hat{p}(s_0)$, $0 < \hat{p}(s_0) < 1$, of this polynomial equation provides an estimate for p_c, the accuracy of which increases with s_0. For the square lattice, the cluster numbers g_{st} and $\bar{g}_{st}$ are known up to $s = 12$ [24] and we calculated $\hat{p}(s_0)$ for $s_0 = 0, \ldots, 12$. Figure 5 shows how $\hat{p}(s_0)$ approaches p_c with increasing s_0. The Zeta functions $\zeta(\tau, s_0)$ and $\zeta(\tau - 1, s_0)$ can be approximated by integrals and their ratio evaluates to $(\tau - 2)(\tau - 1)^{-1}(s_0 + 1)^{-1}$. In many cases corrections for small

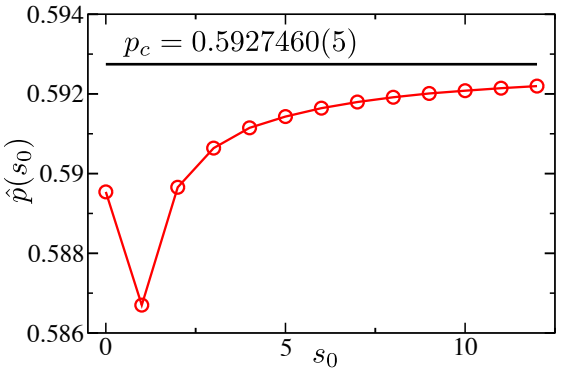

Figure 5. Square lattice – site percolation: The solution $\hat{p}(s_0)$ of Equation 17 approaches p_c with increasing s_0.

Table 1. The deviation of the estimate $\hat{p}(s_0, \Lambda)$ from $p_c(\Lambda)$ decreases rapidly when s_0 is increased from zero to two.

s_0	6^3	$4, 8^2$	$4, 6, 12$	$3, 12^2$	$\frac{1}{2}\binom{3,4,3,12}{3,12^2}$
0	-0.01027	-0.02258	-0.03184	-0.04543	-0.05085
1	-0.00553	-0.00901	-0.01530	-0.01240	-0.02093
2	-0.00551	-0.00283	-0.00701	-0.00615	-0.00937

clusters are not even necessary, and using $s_0 = 0$ and the approximation for the Zeta function yields the simple equation

$$\chi(p) = \frac{\tau - 2}{\tau - 1}(2p - 1), \tag{18}$$

with a unique solution p^*, $0 < p^* < 1$. For all lattices discussed so far, p^* is a fairly accurate estimate of p_c, as shown in the Figures 3 and 4§. Further examples may be found in the supplementary note. Among the lattices studied here, the deviation of p^* from p_c was greatest for the lattices with very high percolation thresholds (comp. Figure 3a and Figure 3b) which are inhomogeneous on small scales. To test whether these deviations are caused by the smallest clusters and holes, we enumerated the clusters and holes of size one and two for the hexagonal lattice, the $(4, 8^2)$ lattice, the $(4, 6, 12)$ lattice, the $(3, 12^2)$ lattice, and the 2-uniform lattice with vertex configuration $\frac{1}{2}(3, 4, 3, 12) + \frac{1}{2}(3, 12^2)$. The deviation of $\hat{p}(s_0)$ from p_c decreases when the contributions of the smallest clusters and holes are subtracted, i.e. s_0 is increased from 0 to 2, see Table 1.

The estimation of the threshold value p_c via Equation 18 will fail, if small clusters or small holes are much more abundant at the critical point than an extrapolation of the asymptotic law for large clusters would suggest. In particular, this is obvious for lattices that contain a substructure which does not contribute to large scale connectivity but dominates the density of small clusters.

§ In many cases, the integral approximation of the Zeta function yields better results than the exact ratio, which is probably due to a subtle cancelation of errors.

4. Three dimensional lattices

The combinatorial EC of percolation patterns P on a d-dimensional lattice is given by the alternating sum of the numbers of k-dimensional lattice cells, $k = 0, \ldots, d$, contained in P. Thus, in the case $d = 3$, the Equation 4 is replaced by

$$\mathcal{X}(P) = \#v - \#e + \#f - \#c, \tag{19}$$

where $\#c$ is the number of black three-dimensional polyhedral lattice cells. The resulting MEC of black clusters in the case of site-percolation on a simple cubic (sc) lattice, for example, is given by

$$\chi_{sc}(p) = p - 3p^2 + 3p^4 - p^8. \tag{20}$$

The black vertices are connected, i.e. they are part of the same cluster, if they are joined by a path of black nearest neighbors on the lattice. As in the two dimensional case, the black clusters partition the white vertices into an aggregate of clusters with a complementary connectivity, such that there is a one-to-one correspondence between cavities in black clusters and finite white clusters, as well as between the cavities in white clusters and finite black clusters. A white vertex of the simple cubic lattice, for example, is connected to all 26 vertices on the boundary of the eight surrounding lattice cubes, in contrast to the six neighbors of the black vertices, which correspond to lattice bonds. In addition to cavities, black clusters can have handles, i.e. they can be homeomorph to a solid torus or objects of higher genus. Each handle of a black cluster is pierced by precisely one handle of a white cluster. From these duality relations and the 3d analogue of Equation 3

$$\mathcal{X}(P) = \#\text{clusters} - \#\text{handles} + \#\text{cavities}, \tag{21}$$

we see that EC of white clusters is identical to that of black clusters. Hence, MEC of white clusters is $\bar{\chi}(\bar{p}) = \chi(1 - \bar{p})$ with $\bar{p} = 1 - p$.

The graph of $\chi_{sc}(p)$ shown in Figure 6 is typical for the MECs in $d = 3$, where the MECs have two distinct non-trivial zero crossings p_0^b and $1 - p_0^w$. In the intermediate regime where $\chi(p) < 0$, the MEC is dominated by interwoven white and black handles. The percolation thresholds of the lattice with black p_c^b and white p_c^w connectivity are different in general. In the range $p_c^b < p < 1 - p_c^w$ a single infinite black cluster coexists with a single infinite white cluster. In order to check for a possible link between zero crossings of $\chi(p)$ and thresholds we compare p_0^b and p_0^w with simulation values p_c^b and p_c^w for the sc lattice, face-centered-cubic (fcc) lattice and the body-centered-cubic (bcc) lattice. The calculation of the MECs for fcc and bcc lattices is reported in the supplementary note. As the Figure 6 already indicates, p_0^b and p_0^w are both upper bounds for p_c^b and p_c^w, and they are becoming tighter as the (effective) coordination numbers increase. The task to device a threshold estimator based on the above findings appears to be more difficult than in the two dimensional case, and it is left for future work.

5. Continuum percolation

So far, we dealt with the EC of percolating clusters on geometric lattices. Let us finally make a few remarks to indicate that the features of the EC induced by the percolation thresholds persist in the case of continuum percolation. Consider the standard Boolean model where penetrable convex grains are positioned randomly at Poisson distributed points in $\mathbb{R}^d$. The grains may be multidispersed having random

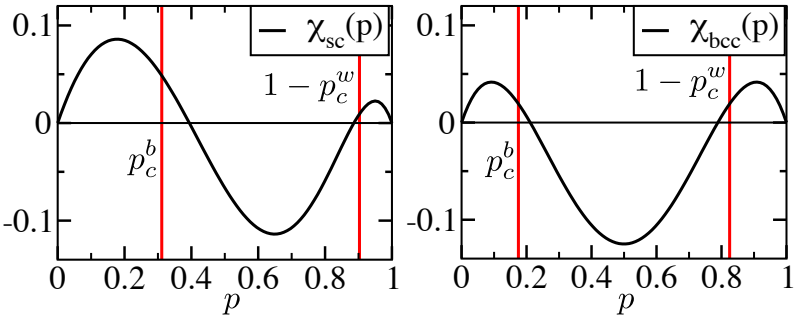

Figure 6. The graphs of the MEC of the simple cubic (sc) and body-centered cubic (bcc) lattice. The bcc lattice has the same black and white connectivities and is hence invariant to the substitution $p = 1 - p$.

Table 2. Numerical values for p_0 and p_c of the cubic lattices for black and white connectivities. The bcc lattice has equal black and white connectivities. Threshold densities are taken from ^{a})[25], ^{b})[26]

lattice	z	p_0	p_c
sc (black)	6	0.3940	0.3116^a
fcc (black)	12	0.2370	0.1992^a
bcc	14	0.2113	0.175^b
fcc (white)	18	0.1616	0.136^b
sc (white)	26	0.1139	0.097^b

size, shape and orientation. By using results from integral geometry, the MEC of patterns formed by clusters of overlapping grains can be calculated exactly [27]. In $d = 2$ the MEC reads

$$\chi_2(\eta) = \eta(I - \eta)e^{-\eta}, \quad \eta = \rho a, \tag{22}$$

with the grain density ρ, and the dimensionless ratio $I = \frac{u}{4\pi a}$; a and u denote the average grain area and perimeter, both assumed to be distributed independently from the grain locations. In the case of monodispersed convex grains, $I \geq 1$ is an isoperimetric ratio. For $d = 3$ one finds

$$\chi_3(\zeta) = (1 - 3I_1\zeta + \frac{3\pi^2}{32} I_2\zeta^2)e^{-\zeta}, \quad \zeta = \rho v. \tag{23}$$

Here, $I_1 = \frac{sb}{6v}$, $I_2 = \frac{s^3}{36\pi v^2}$; b, s and v are the averages of the grain mean breadth, surface area and volume, respectively. Again, for monodispersed convex grains, $I_1 \geq 1$, $I_2 \geq 1$. The graphs of $\chi(p)$ and $\bar{\chi}(p)$, when plotted as functions of the mean coverage $0 \leq 1 - e^{-\eta} < 1$ and $0 \leq 1 - e^{-\zeta} < 1$ are similar to the graphs of the corresponding lattice MECs: $\chi_2(\eta)$ has a single zero at $\eta_0 = I^{-1}$, $\chi_3(\zeta)$ has two zeros located at $\zeta_0 = \frac{96}{\pi}\frac{bv}{s^2}\left(1 \pm \sqrt{1 - \frac{\pi}{24}\frac{s}{b^2}}\right)$. For monodispersed discs $\eta_0 = 1$, which may be compared with the threshold value $\eta_c \approx 1.12$. Monodispersed spheres yield $\zeta_0^- = 0.377$, to be compared with the percolation threshold of penetrable spheres, $\zeta_c \approx 0.34$ [28]. The interpretation of the continuum MECs in terms of cluster structures can be carried over unchanged from the lattice examples. Thus, for instance, ζ_0^+ is expected to provide a quick estimate for the percolation threshold ζ_c^+ of the void space defined as the set complement of the pattern by the clusters of overlapping grains.

6. Summary and Discussion

Taken together, the equations (17) and (18) represent our main result. The relation (18) connects the universal scaling behaviour of percolating clusters at p_c with their specific topological structure, as expressed by the mean Euler characteristic. It provides a novel and parameter-free estimate of threshold values for two-dimensional lattices, which is remarkably accurate. In the case of self-matching lattices Eq.(18) reproduces the exact values $p_c = 1/2$, and offers an explanation for the numerical finding that the zero crossing of the MEC, p_0, is a tight upper (lower) bound for the threshold p_c if $p_c > 1/2$ ($p_c < 1/2$).

Over the years, a variety of "universal" approximate formulae for predicting percolation thresholds have been devised [14, 29, 30, 31]. Most of these proposals fit an empirical relation with a number of free parameters to a set of known thresholds. Recently, Wierman and Naor [32] introduced a list of criteria for the evaluation of such formulae. Accordingly, these should (1) be well defined, (2) be easily computable, (3) provide values only between 0 and 1, (4) depend only on the adjacency structure of the lattice, (5) be accurate, (6) be consistent with the matching relationship, and (7) be consistent with the containment principle.

The Eq.(18) complies with the first six of these requirements, as can be inferred from its deduction and from the comparision of our estimates with precise numerical threshold values. We have not checked in detail the criterion (7). The claim, that our p_c-estimation is well defined may perhaps be questioned, since Eq.(18) involves an extrapolation of the scaling ansatz to the smallest cluster sizes. However, this ad hoc simplification can be removed by going back to the "master equation" (17), which provides means to systematically correct for small-scale irregularities, as shown in Table 1.

We mentioned the exact expressions of the mean Euler characteristic for 3d-cubic lattices and for the Boolean model of continuum percolation in two and three dimensions. The close linking of the zero crossings of these MECs to the respective threshold densities appears to persist and underlines once more the role of the Euler characteristic as the appropriate concept for describing the topological aspects of percolation. But to apply this intriguing fact for the construction of threshold estimators for three dimensions and for continuum models remains a challenging problem.

Acknowledgments

We would like to thank Robert Ziff for valuable comments on the manuscript. RAN acknowledges financial support by the DFG and the state of Bavaria via IDK-NBT.

References

[1] MB Isichenko. Percolation, statistical topography, and transport in random media. 1992. *Rev. Mod. Phys.*, 64:961.

[2] M. E. J. Newman. Spread of epidemic disease on networks. 2002. *Phys. Rev. E*, 66(1):016128. doi: 10.1103/PhysRevE.66.016128.

[3] S Fortunato and H Satz. Polyakov loop percolation and deconfinement in SU(2) gauge theory. 2000. *Phys. Lett. B*, 475:311.

[4] B. D. Hughes. *Random Walks and Random Environments*, volume 2. Oxford Science Publications, 1996.

[5] D. Stauffer and A. Aharony. *Perkolationstheorie*. VCH, 1995.

[6] G. R. Grimmett. *Percolation*. Springer, 1999.

[7] M. F. Sykes and J. W. Essam. Some exact critical percolation probabilities for bond and site problems in two dimensions. 1963. *Phys. Rev. Lett.*, 10(1):3–4.

[8] H Kesten. The critical probability of bond percolation on the square lattice equals $\frac{1}{2}$. 1980. *Comm. Math. Phys.*, 74:41–59.

[9] J C Wierman. A bond percolation critical probability determination based on the star-triangle transformation. 1984. *Journal of Physics A: Mathematical and General*, 17(7):1525–1530.

[10] Robert M. Ziff. Generalized cell–dual-cell transformation and exact thresholds for percolation. 2006. *Phys. Rev. E*, 73(1):016134. doi: 10.1103/PhysRevE.73.016134.

[11] Christian R. Scullard. Exact site percolation thresholds using a site-to-bond transformation and the star-triangle transformation. 2006. *Phys. Rev. E*, 73(1):016107. doi: 10.1103/PhysRevE.73.016107.

[12] F. Y. Wu. New critical frontiers for the potts and percolation models. 2006. *Phys. Rev. Lett.*, 96(9):090602. doi: 10.1103/PhysRevLett.96.090602.

[13] M.F. Sykes and J.W. Essam. Exact critical percolation probabilities for site and bond problems in two dimensions. 1964. *J. of Math. Phys.*, 5:1117–1127.

[14] P.N. Suding and R.M. Ziff. Site percolation thresholds for Archimedean lattices. 1999. *Phys. Rev. E*, 60:275–283.

[15] Robert Parviainen. Estimation of bond percolation thresholds on the Archimedean lattices, 2007. *J. Phys. A*, 40:9253-9258.

[16] S. van der Marck. The site and bond percolation thresholds of the Archimedean lattices and their duals. private communication, 2003.

[17] Grünbaum and Shephard. *Tilings and Patterns*. W. H. Freeman and Company, 1986.

[18] M.E.J. Newman and R.M. Ziff. Fast Monte Carlo algorithm for site or bond percolation. 2001. *Phys. Rev. E*, 64:016706.

[19] J.W. Essam. Potts models, percolation, and duality. 1979. *J. of Math. Phys.*, 20:1769–1773.

[20] Michael E. Fisher. Critical probabilities for cluster size and percolation problems. 1961. *Journal of Mathematical Physics*, 2(4):620–627. doi: 10.1063/1.1703746.

[21] D. Stauffer. Scaling theory of percolation clusters. 1979. *Physics Reports*, 54(1):1–74.

[22] B Nienhuis, E K Riedel, and M Schick. Magnetic exponents of the two-dimensional q-state potts model. 1980. *Journal of Physics A: Mathematical and General*, 13(6):L189–L192.

[23] Stanislas Smirnov and Wendelin Werner. Critical exponents for two-dimensional percolation. 2001. *Math. Res. Lett*, 8:729.

[24] Stephan Mertens. Lattice animals: A fast enumeration algorithm and new perimeter polynomials. 1990. *J. Stat. Phys.*, 58(5/6):1095–1108.

[25] Christian D Lorenz and Robert M Ziff. Universality of the excess number of clusters and the crossing probability function in three-dimensional percolation. 1998. *Journal of Physics A: Mathematical and General*, 31(40):8147–8157.

[26] J. W. Essam. Percolation and cluster size. In C. Domb and M. S. Green, editors, *Phase Transition and Critical Phenomena*, volume 2, pages 197–270. Academic Press London, 1972.

[27] K. R. Mecke and H. Wagner. Euler characteristic and related measures for random geometric sets. 1991. *J. Stat. Phys.*, 64:843.

[28] Christian D. Lorenz and Robert M. Ziff. Precise determination of the critical percolation threshold for the three-dimensional "swiss cheese" model using a growth algorithm. 2001. *The Journal of Chemical Physics*, 114(8):3659–3661. doi: 10.1063/1.1338506.

[29] Harvey Scher and Richard Zallen. Critical density in percolation processes. 1970. *The Journal of Chemical Physics*, 53(9):3759–3761. doi: 10.1063/1.1674565.

[30] Serge Galam and Alain Mauger. Universal formulas for percolation thresholds. 1996. *Phys. Rev. E*, 53(3):2177–2181. doi: 10.1103/PhysRevE.53.2177.

[31] John C. Wierman, Dora Passen Naor, and Rulian Cheng. Improved site percolation threshold universal formula for two-dimensional matching lattices. 2005. *Phys. Rev. E*, 72(6):066116.

[32] John C. Wierman and Dora Passen Naor. Criteria for evaluation of universal formulas for percolation thresholds. 2005. *Phys. Rev. E*, 71(3):036143.